Обзор ArXiv/astro-ph, 11-16 марта 2026

От Сильченко О.К.

ArXiv: 2603.06913

Imaging the disk-halo interface of NGC 891: a 2.7 kpc-thick molecular gas disk

D. Jiménez-López, S. García-Burillo, M. Querejeta, A. Usero, P. Tarrío

Observatorio Astronómico Nacional, Madrid, Spain
e-mail: d.jimenez@oan.es, s.gburillo@oan.es, m.querejeta@oan.es, a.usero@oan.es, p.tarrio@oan.es

ABSTRACT

Context. Halos surrounding spiral galaxies act as the bridges connecting the galactic disk and the intergalactic medium (IGM). They host a significant fraction of the baryonic mass in the Universe, and feedback from star formation (SF) or active galactic nuclei (AGN) likely plays an important role in regulating this vertical baryonic component. Despite its importance, the contribution of extraplanar molecular gas remains poorly understood.
Aims. We aim to characterize the vertical extent and the kinematics of molecular gas traced by CO(2-1) emission in the nearby (D = 9.5 Mpc) spiral galaxy NGC 891, one of the best studied edge-on galaxies. We also compare our results with the extraplanar distribution of other tracers of baryonic matter, including atomic gas (HI), diffuse ionized gas (Hα-traced DIG), and dust maps from the literature.
Methods. Our analysis is based on new CO(2–1) observations of NGC 891 obtained with the IRAM 30m telescope. We mapped two 6 kpc $\times$ 6 kpc regions on the northeastern side and the area surrounding the galactic center. We apply a careful method to estimate and remove the residual contribution of the error beam to the CO cube.
Results. The vertical extent of the molecular gas is best described by a two-component Gaussian fit, consisting of a bright thin disk component (deconvolved $FWHM \simeq 360$ pc) and a fainter thick disk component (deconvolved $FWHM \simeq 1.1$ kpc). Statistically significant ($> 3\sigma$) CO(2-1) emission is detected up to 1.3-1.4 kpc above the disk midplane. We estimate that the thick molecular disk component contains up to $\sim 27\%$ of the total molecular gas mass of the galaxy. The vertical extent of Hα emission is similar to that of the molecular gas, whereas HI extends much further.
Conclusions. Our results demonstrate that SF-driven feedback in a non-starburst galaxy can lift significant amounts of molecular gas to large vertical distances. We interpret the presence of extraplanar molecular gas in NGC 891 in the framework of a galactic fountain scenario, in which material is expelled from star-forming regions and transported toward the outer halo. This is supported by optical images where dust columns rise from the inner disk, showing spatial correlation between CO (2-1), Hα, and dust.

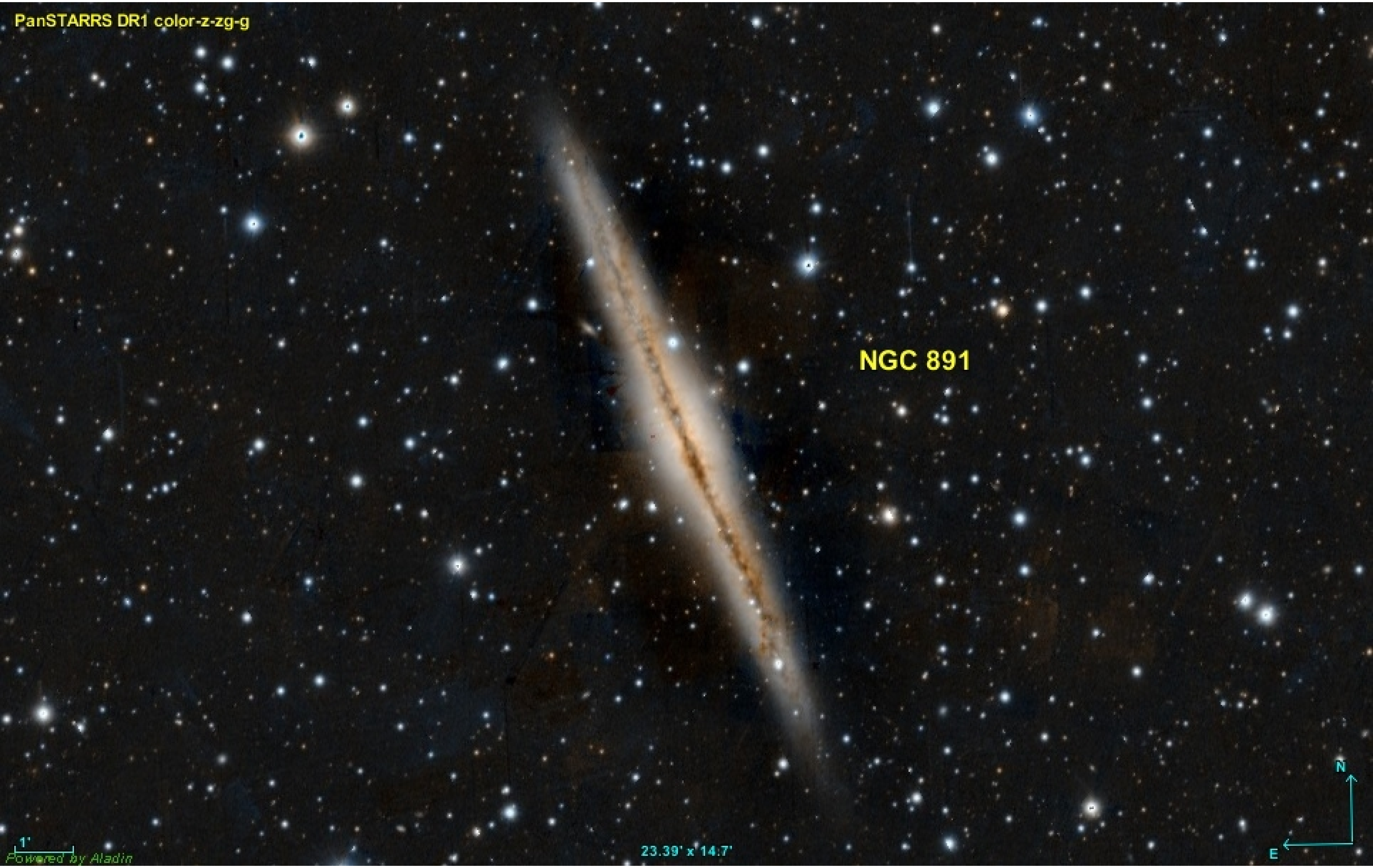
PanSTARRS DR1 color-z-zg-g
NGC 891
N
E
1'
23.39' x 14.7'
Powered by Aladin

Данные

- ALMA, CO, с разрешением 0.5 кпк
- Архивные данные HI, WSRT
- Архивные данные в оптической эмиссии H-alpha, Fabry-Perot, WHT

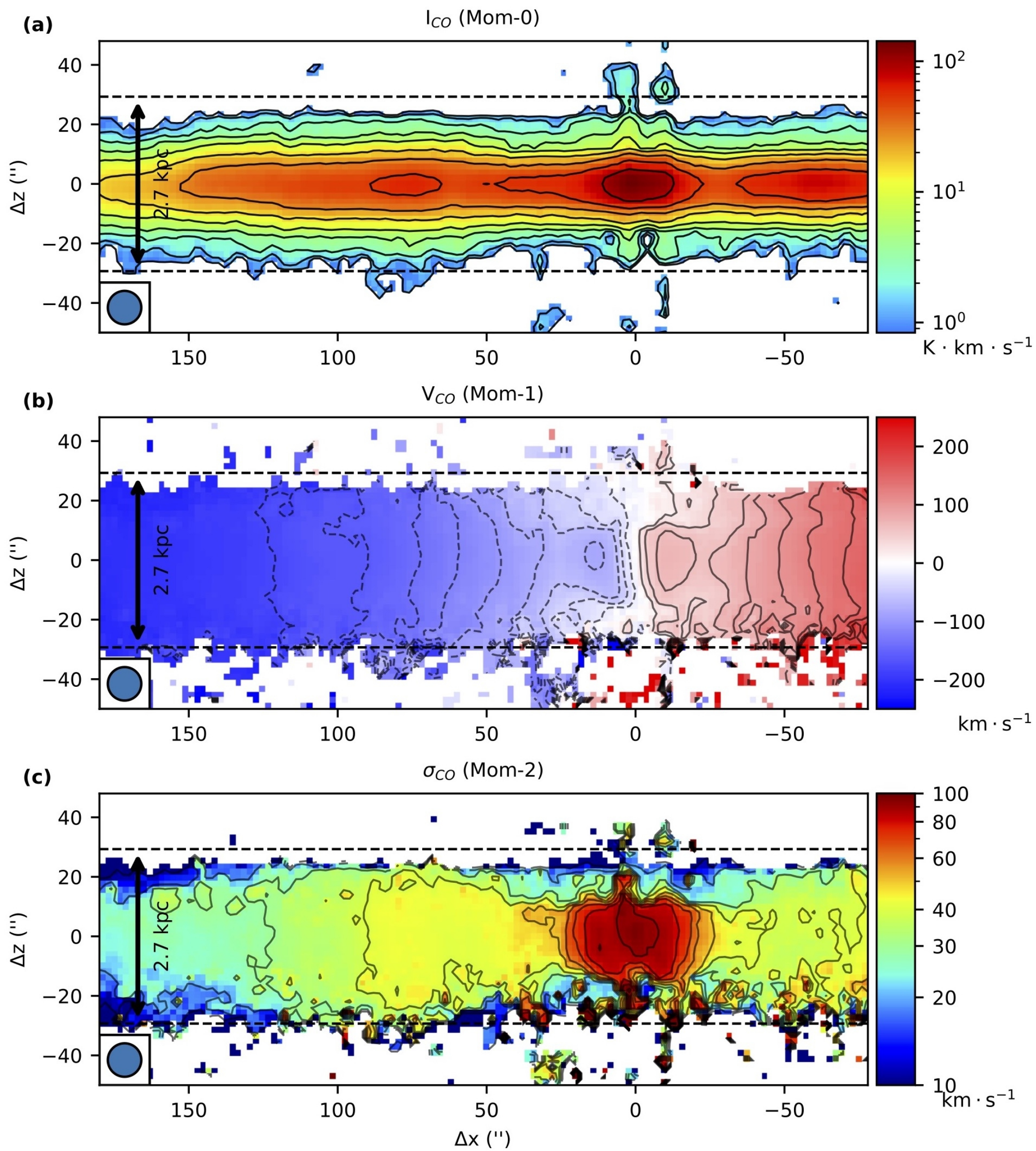

Fig. 3. CO moment maps. From top to bottom: the velocity-integrated intensities (*panel a)*), the intensity-weighted velocities (*panel b*) and the velocity dispersions (*panel c*) derived from the CO(2–1) line in the mapped region. Contour levels for the CO intensities increase logarithmically from 3σ to 600σ in steps of 0.26 dex, with σ = 0.28 K km s^{-1}. Mean-velocity contours range from -180 to 180 km s^{-1} in steps of 20 km s^{-1}. Dashed lines indicate negative contour values. Dispersion contours go from 10 to 100 km s^{-1} in steps of 10 km s^{-1}. The 30 m beam size (11.2″) is indicated as a filled circle in the bottom left corner of each panel. A vertical thickness of 2.7 kpc is represented as horizontal dashed lines, as visual reference.

Комбинация двух дисков молекулярного газа: тонкого и толстого

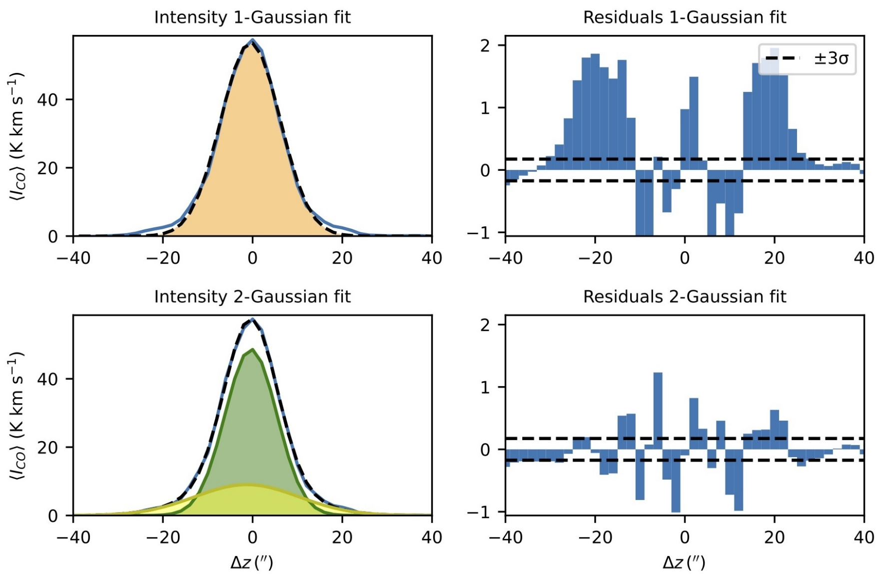

Fig. 5. Comparison of the average out-of-plane distribution of CO (<I_{CO}>(Δz)) with the fits of the single-Gaussian (*upper panels*) and double-Gaussian (*lower panels*) decomposition models described in Sect. 4.2. The blue curve shows the observed profile <I_{CO}>(Δz). The green and yellow curves in the *lower left panel* show the fit of the thin and thick molecular disk components of the double-Gaussian fit, respectively. The black dashed curves represent the sum of all the components in both models. The *upper* and *lower right panels* display the residuals of the fits. Horizontal dashed lines indicate the $\pm 3\sigma$ levels with σ = 58 mK km s^{-1}.

	CO (2-1)	HI	H_α
A_{1G}	0.970 ± 0.008	0.823 ± 0.009	0.95 ± 0.01
$FWHM_{1G}$ [kpc]	0.49 ± 0.01	1.49 ± 0.02	1.25 ± 0.02
$\Delta z_{3\sigma}$ [kpc]	2.07	4.45	3.12
A_{2G}	1.008 ± 0.006	0.956 ± 0.004	0.995 ± 0.006
A_{thin}	0.73 ± 0.04	0.586 ± 0.006	0.19 ± 0.01
A_{thick}	0.27 ± 0.04	0.414 ± 0.006	0.81 ± 0.01
$FWHM_{thin}$ [kpc]	0.36 ± 0.02	1.15 ± 0.01	0.53 ± 0.02
$FWHM_{thick}$ [kpc]	1.1 ± 0.1	3.91 ± 0.07	1.60 ± 0.02
$\Delta z_{thick,3\sigma}$ [kpc]	3	10	3.8

Table 2. Results obtained from the single-Gaussian (1G) and double-Gaussian (2G) fits of the average out-of-plane profiles of CO, HI and Hα. $A_{1G,2G}$ represent the fraction of the observed flux in the profiles that is accounted for by the fitted components, $FWHM_{1G,2G}$ are the deconvolved full widths at half maximum of each component, $\Delta z_{3\sigma}$ are the full widths of the fitted components measured at a 3σ level. The table also includes the values for the parameters of the thin and thick Gaussian fitting curves of the two-components model.

Сравнение трех дисков

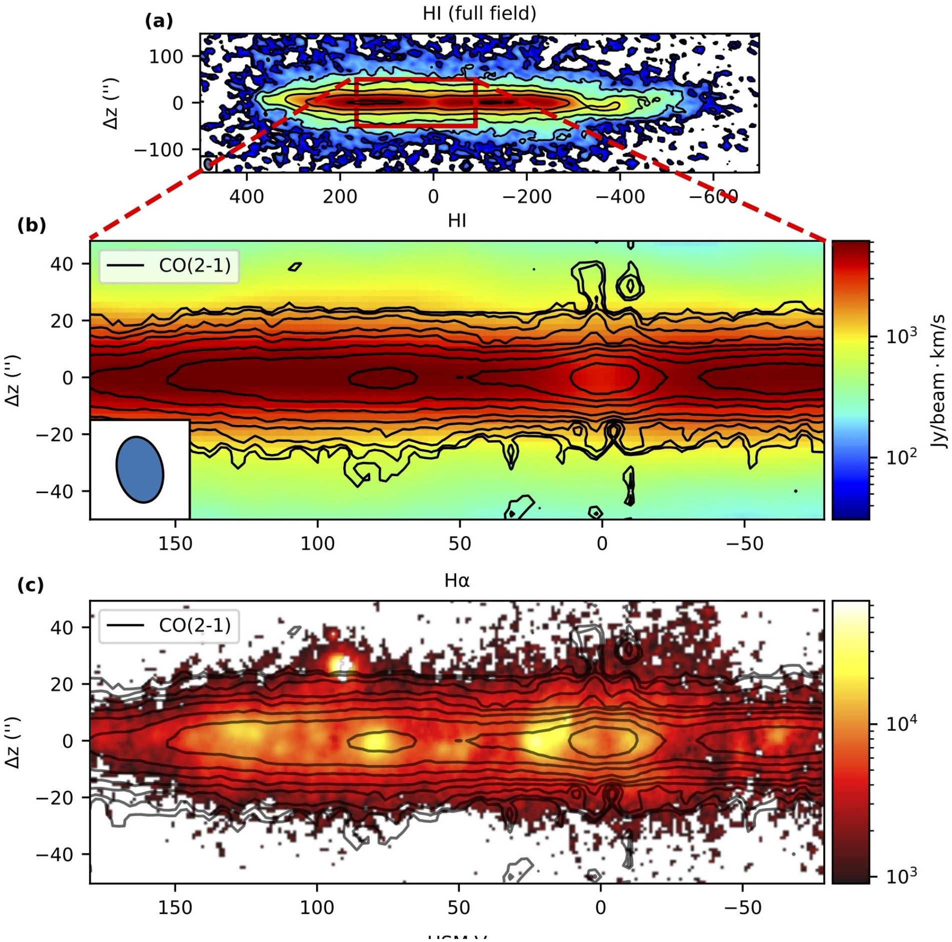

	CO (2-1)	HI	H_α
A_{1G}	0.970 ± 0.008	0.823 ± 0.009	0.95 ± 0.01
$FWHM_{1G}$ [kpc]	0.49 ± 0.01	1.49 ± 0.02	1.25 ± 0.02
$\Delta z_{3\sigma}$ [kpc]	2.07	4.45	3.12
A_{2G}	1.008 ± 0.006	0.956 ± 0.004	0.995 ± 0.006
A_{thin}	0.73 ± 0.04	0.586 ± 0.006	0.19 ± 0.01
A_{thick}	0.27 ± 0.04	0.414 ± 0.006	0.81 ± 0.01
$FWHM_{thin}$ [kpc]	0.36 ± 0.02	1.15 ± 0.01	0.53 ± 0.02
$FWHM_{thick}$ [kpc]	1.1 ± 0.1	3.91 ± 0.07	1.60 ± 0.02
$\Delta z_{thick,3\sigma}$ [kpc]	3	10	3.8

Table 2. Results obtained from the single-Gaussian (1G) and double-Gaussian (2G) fits of the average out-of-plane profiles of CO, HI and Hα. $A_{1G,2G}$ represent the fraction of the observed flux in the profiles that is accounted for by the fitted components, $FWHM_{1G,2G}$ are the de-convolved full widths at half maximum of each component, $\Delta z_{3\sigma}$ are the full widths of the fitted components measured at a 3σ level. The table also includes the values for the parameters of the thin and thick Gaussian fitting curves of the two-components model.

Сравнение трех дисков

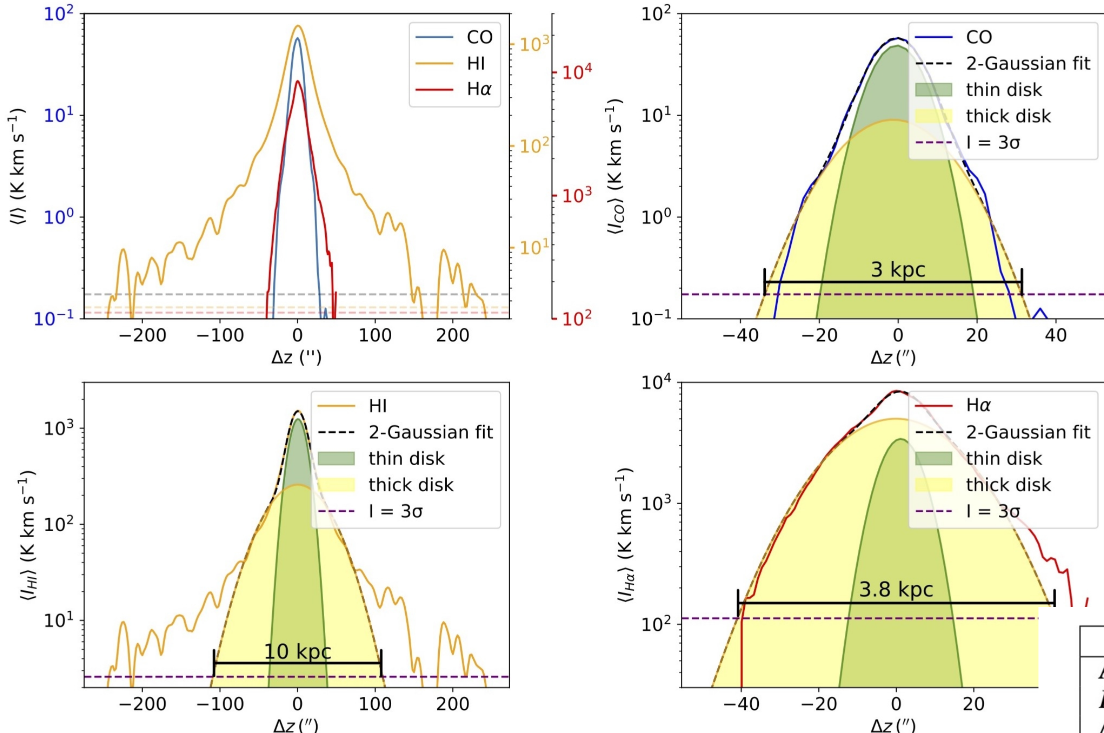

Fig. 7. *Upper left panel*: Comparison of the average out-of-plane profiles of CO, HI, and Hα. All panels display the y-axis in loga
The integration ranges over the x-axis used to derive the profiles [Δx_{min}, Δx_{max}] are: [180″, -80″] for CO, [1150″, -1050″] for HI, and
for Hα. *Upper right panel*: Results of the double-Gaussian fit (black dashed line) of the CO profile (blue solid line). The thin disk a
Gaussian components are shown in green and yellow lines, respectively. *Lower panels*: Same as *Upper right panel* but for the HI anc
Horizontal dashed lines show the 3σ thresholds for each tracer in all panels (σ_{CO} = 58 mK km s^{-1}, σ_{HI} = 864 mK km s^{-1}, and $\sigma_{H\alpha}$ =

	CO (2-1)	HI	H_α
A_{1G}	0.970 ± 0.008	0.823 ± 0.009	0.95 ± 0.01
$FWHM_{1G}$ [kpc]	0.49 ± 0.01	1.49 ± 0.02	1.25 ± 0.02
$\Delta z_{3\sigma}$ [kpc]	2.07	4.45	3.12
A_{2G}	1.008 ± 0.006	0.956 ± 0.004	0.995 ± 0.006
A_{thin}	0.73 ± 0.04	0.586 ± 0.006	0.19 ± 0.01
A_{thick}	0.27 ± 0.04	0.414 ± 0.006	0.81 ± 0.01
$FWHM_{thin}$ [kpc]	0.36 ± 0.02	1.15 ± 0.01	0.53 ± 0.02
$FWHM_{thick}$ [kpc]	1.1 ± 0.1	3.91 ± 0.07	1.60 ± 0.02
$\Delta z_{thick,3\sigma}$ [kpc]	3	10	3.8

Table 2. Results obtained from the single-Gaussian (1G) and double-Gaussian (2G) fits of the average out-of-plane profiles of CO, HI and Hα. $A_{1G,2G}$ represent the fraction of the observed flux in the profiles that is accounted for by the fitted components, $FWHM_{1G,2G}$ are the deconvolved full widths at half maximum of each component, $\Delta\ z_{3\sigma}$ are the full widths of the fitted components measured at a 3σ level. The table also includes the values for the parameters of the thin and thick Gaussian fitting curves of the two-components model.

По скоростям: в толстом молекулярном диске нет лага

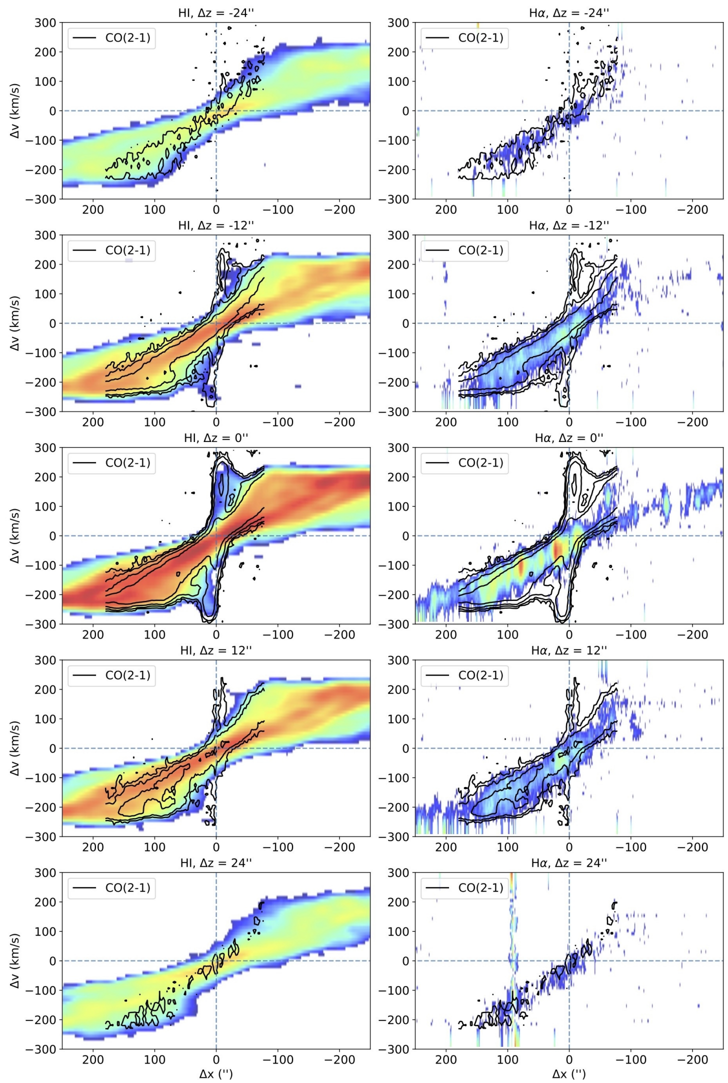

Fig. 9. PV slices parallel to the galactic plane of the HI (left) and Hα (right) emissions. Slices are taken at $\Delta z = 0''$, $12''$and $24''$above and below the midplane. Color scales are clipped at $3\,\sigma_{\rm ch}$ ($\sigma_{\rm ch,HI} = 147$ mK, $\sigma_{\rm ch,H\alpha} = 3.8$ K). PV slices of the CO(2-1) emission are plotted as black contours, with levels $3\sigma_{\rm ch,CO}$, $9\sigma_{\rm ch,CO}$, $27\sigma_{\rm ch,CO}$ and $81\sigma_{\rm ch,CO}$ ($\sigma_{\rm ch,CO} = 3.5$ mK). Dashed blue lines denote the zero-offset coordinates.

ArXiv: 2603.12945

WISDOM Project – XXVIII. Molecular gas measurement of the supermassive black hole mass of the galaxy NGC 1387

Pandora Dominiak,[1★] Martin Bureau,[1†] Fu-Heng Liang,[1,2,3] Michele Cappellari,[1] Timothy A. Davis,[4] Federico Lelli,[5] Ilaria Ruffa,[4,5] Thomas G. Williams[1,6] and Hengyue Zhang[1]
[1]*Sub-department of Astrophysics, Department of Physics, University of Oxford, Denys Wilkinson Building, Keble Road, Oxford, OX1 3RH, UK*
[2]*European Southern Observatory, Karl-Schwarzschild-Straße 2, Garching 85748, Germany*
[3]*Astronomisches Rechen-Institut, Zentrum für Astronomie der Universität Heidelberg, Mönchhofstraße 12-14, Heidelberg 69120, Germany*
[4]*Cardiff Hub for Astrophysics Research & Technology, School of Physics & Astronomy, Cardiff University, Queens Buildings, Cardiff, CF24 3AA, UK*
[5]*INAF - Arcetri Astrophysical Observatory, Largo Enrico Fermi 5, 50125, Florence, Italy*
[6]*UK ALMA Regional Centre Node, Jodrell Bank Centre for Astrophysics, Department of Physics and Astronomy, The University of Manchester, Oxford Road, Manchester M13 9PL, UK*

Accepted XXX. Received YYY; in original form ZZZ

ABSTRACT

Supermassive black hole (SMBH) masses can be measured using molecular gas kinematics. Here we present high angular resolution (0.12 arcsec or ≈ 11 pc) Atacama Large Millimeter/submillimeter Array observations of the ^{12}CO(2–1) line emission of the early-type galaxy NGC 1387. The observations reveal a face-on, regularly-rotating central molecular gas disc with a diameter of ≈ 18 arcsec (≈ 1.7 kpc) and a central depression slightly larger than the SMBH sphere of influence. We forward model the CO data cube in a Bayesian framework with the Kinematic Molecular Simulation code, and use *Hubble Space Telescope* data to constrain the stellar gravitational potential contribution to the molecular gas kinematics. We infer a SMBH mass of $1.10^{+1.71}_{-0.95}\,[\mathrm{stat}, 3\sigma]\,^{+2.45}_{-1.09}\,[\mathrm{sys}]\times10^{8}\ \mathrm{M}_{\odot}$ and a F160W-filter stellar mass-to-light ratio of $0.90^{+0.44}_{-0.35}\,[\mathrm{stat}, 3\sigma]\,^{+0.46}_{-0.36}\,[\mathrm{sys}]\ \mathrm{M}_{\odot}/\mathrm{L}_{\odot,\mathrm{F160W}}$. This SMBH mass is consistent with the SMBH mass – stellar velocity dispersion relation.

NGC 1387:Из нашей фотометрии

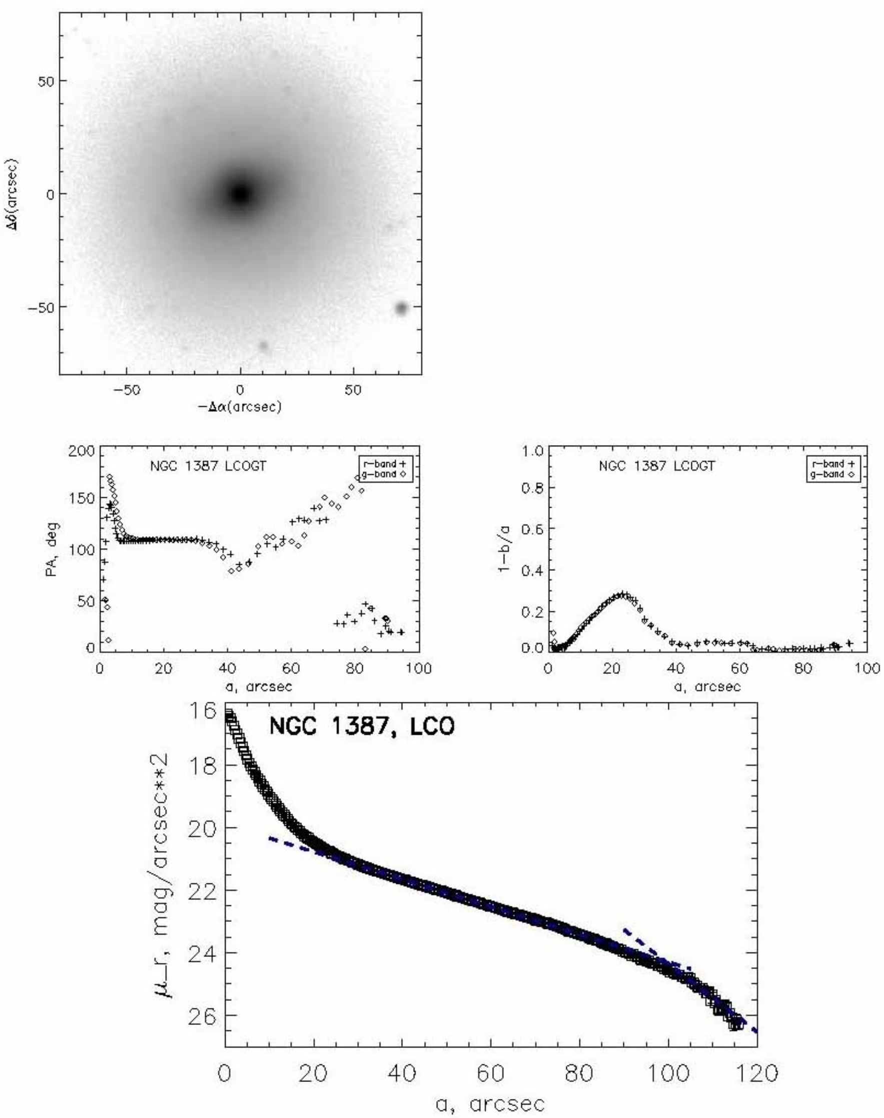

2 NGC 1387

NGC 1387 is a barred lenticular (SB0) galaxy located at $03^{h}36^{m}57\overset{s}{.}06$, $-35°30'23\overset{''}{.}9$ (J2000.0) within the Fornax Cluster. It is located at an angular distance of ≈ 19 arcmin (≈ 107 kpc) to the west of NGC 1399 (Napolitano et al. 2022), the central galaxy of the Fornax Cluster. Throughout this paper we adopt a distance of 19.3 ± 0.8 Mpc, calculated using surface brightness fluctuations (Blakeslee et al. 2009). At this distance, 1 arcsec corresponds to ≈ 94 pc.

NGC 1387 has a total stellar mass of 4.70×10^{10} $M_{\odot}$, derived using an i-band absolute magnitude of −21.81 and a stellar mass-to-light ratio (M/L) in the i-band $M/L_i = 1.31$ $M_{\odot}/L_{\odot,i}$ (Iodice et al. 2019). *Hubble Space Telescope* (*HST*) optical images reveal a prominent central bulge, a weak bar and a face-on dust disc extending ≈ 18 arcsec (≈ 1.7 kpc) in diameter along the major axis, with modest and flocculent dust (see Fig. 1).

Наблюдения с ALMA в CO

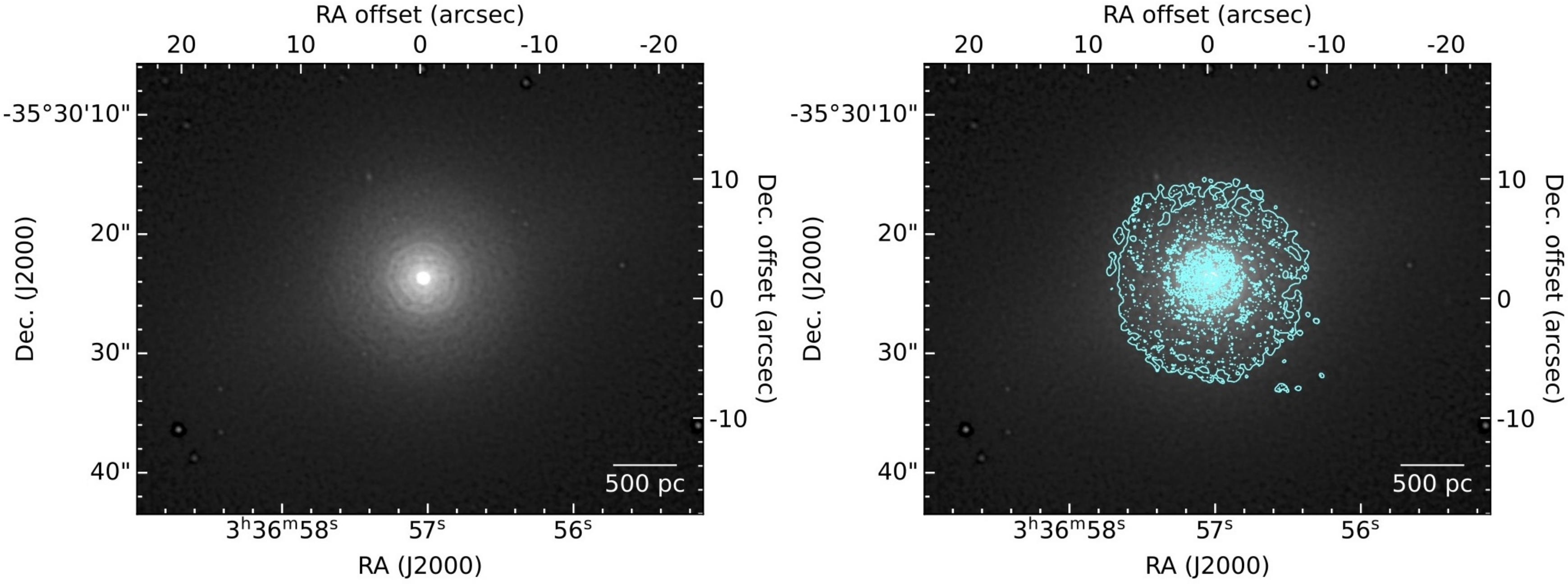

Figure 1. Unsharp-masked *HST* Wide Field Camera 3 F160W-filter (*H*-band) image of NGC 1387 (left), overlaid with the ^{12}CO(2–1) integrated intensity contours (cyan) from our high-resolution ALMA data cube (right). Note that the unsharp masking has removed the smooth outer galaxy light and instead highlights the face-on nuclear disc and bar of the galaxy.

Два разрешения: 0.1" & 0.4"

Результаты высокого разрешения

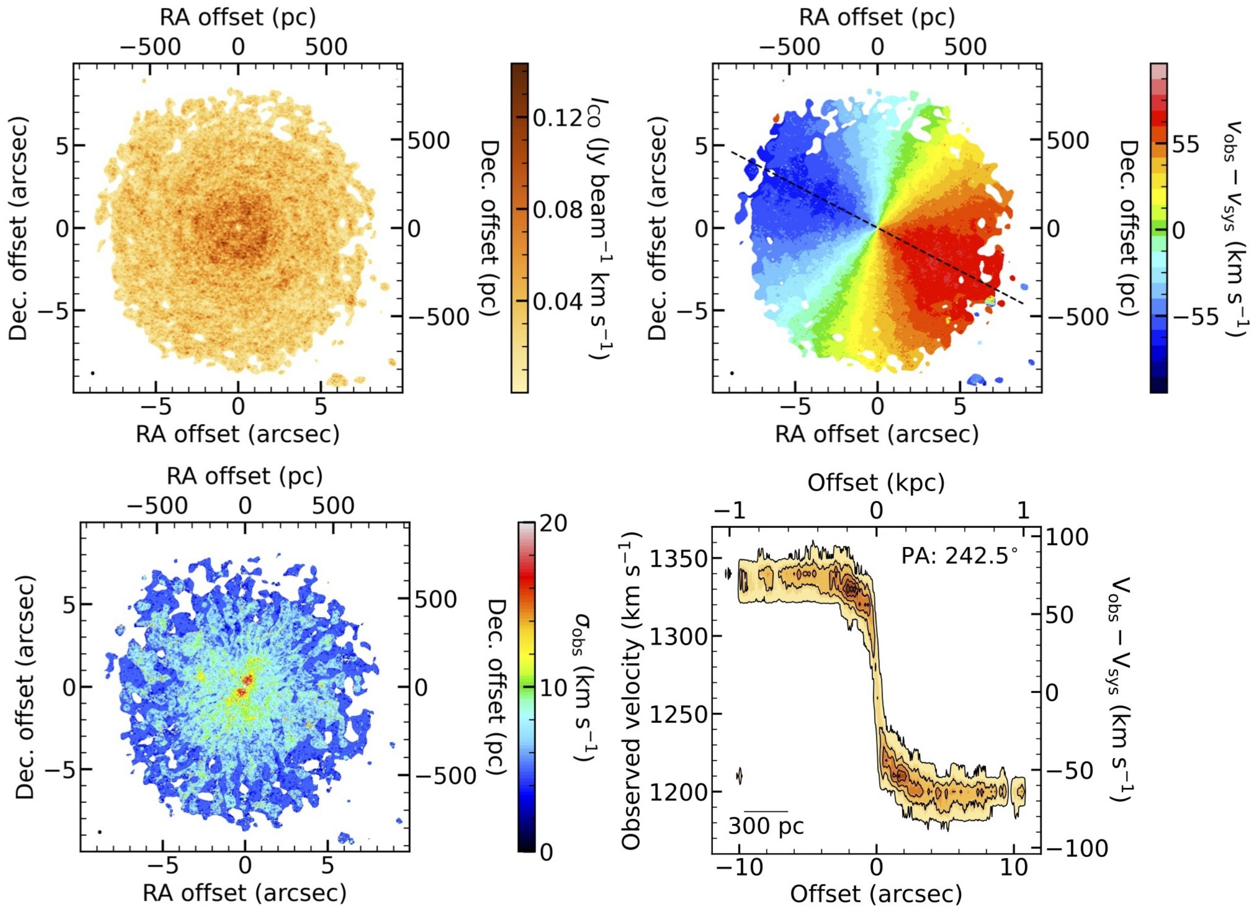

Figure 3. ^{12}CO(2–1) data products of NGC 1387 derived from our ALMA high-resolution data cube. **Top-left:** Zeroth-moment (integrated-intensity) map. **Top-right:** First-moment (intensity-weighted mean line-of-sight velocity) map. The dashed black line shows the kinematic major axis. **Bottom-left:** Second-moment (intensity-weighted line-of-sight velocity dispersion) map. The synthesised beam is shown in the bottom-left corner of each map as a black filled ellipse. **Bottom-right:** Kinematic major-axis position-velocity diagram. An error bar is shown in the bottom-left corner, showing the size of the synthesised beam along the kinematic major axis and the channel width.

CO с низким разрешением

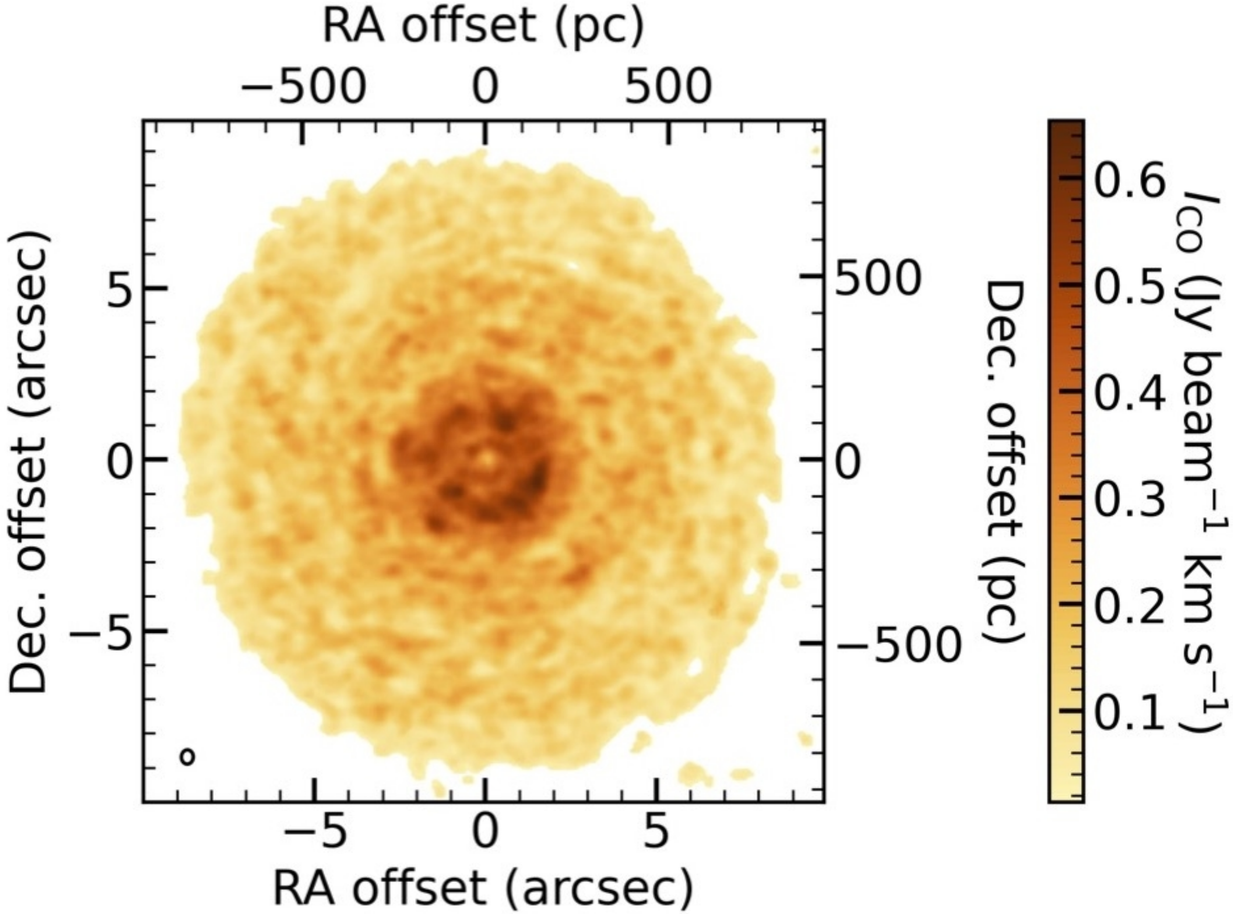

Figure 5. ^{12}CO(2–1) zeroth-moment (integrated-intensity) map of NGC 1387 derived from our ALMA low-resolution data cube. The synthesised beam is shown in the bottom-left corner as a black open ellipse.

Модель звездной массы: MGE

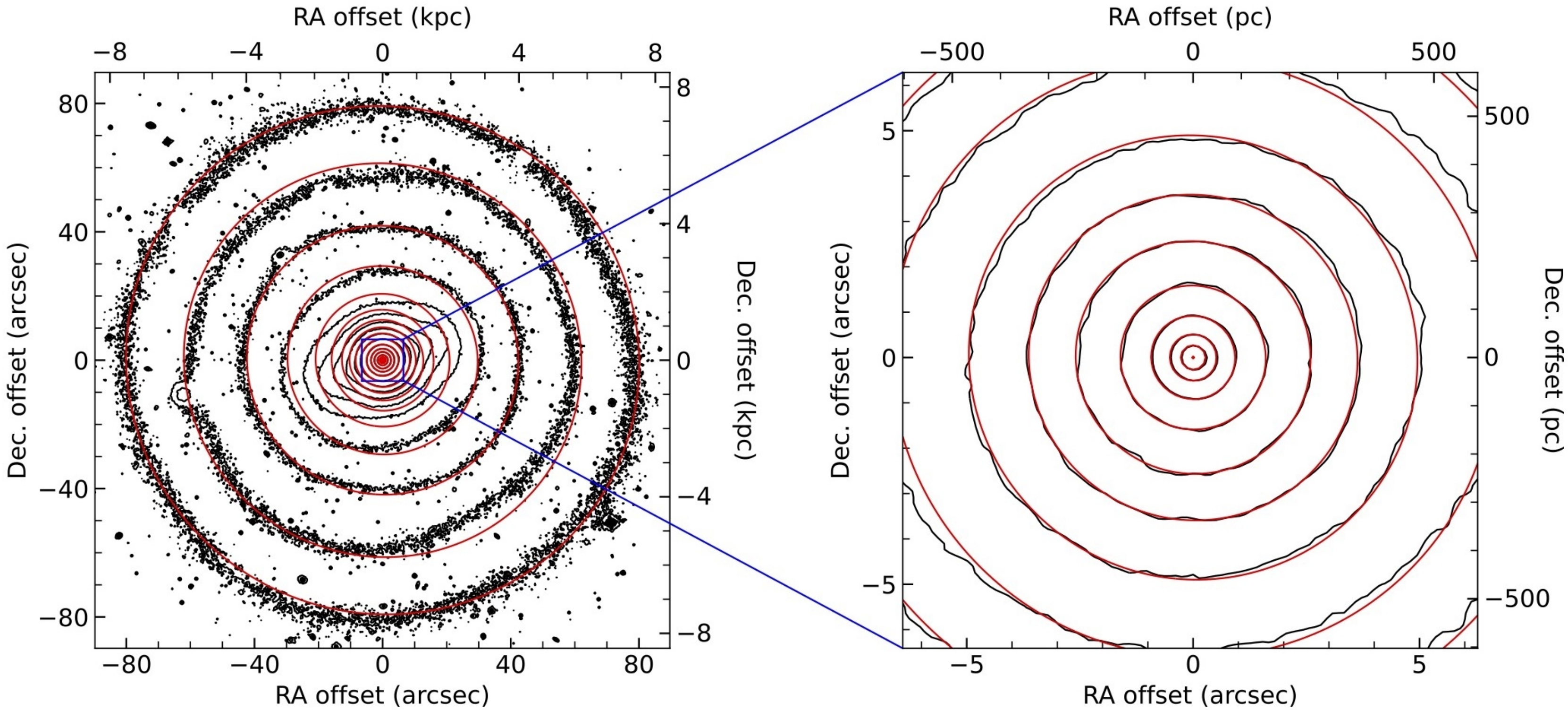

Figure 4. *HST* WFC3 F160W-filter (*H*-band) image of NGC 1387 (black contours), overlaid with our best-fitting MGE model (red contours). **Left:** Full extent of the galaxy, showing the galaxy bulge, bar and extended stellar disc. **Right:** Central region only.

Подгонка свободных параметров

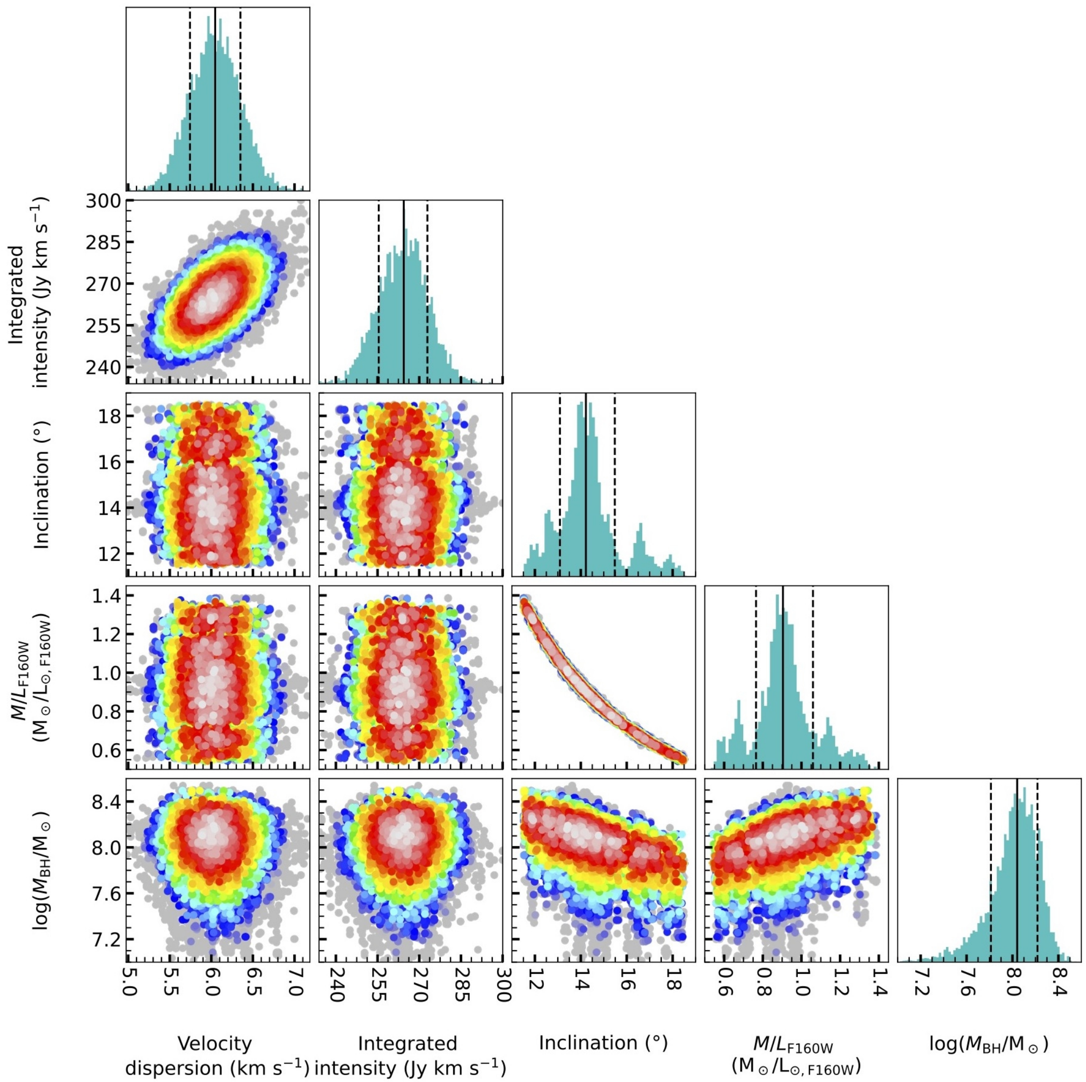

Уверенно обнаружена черная дыра

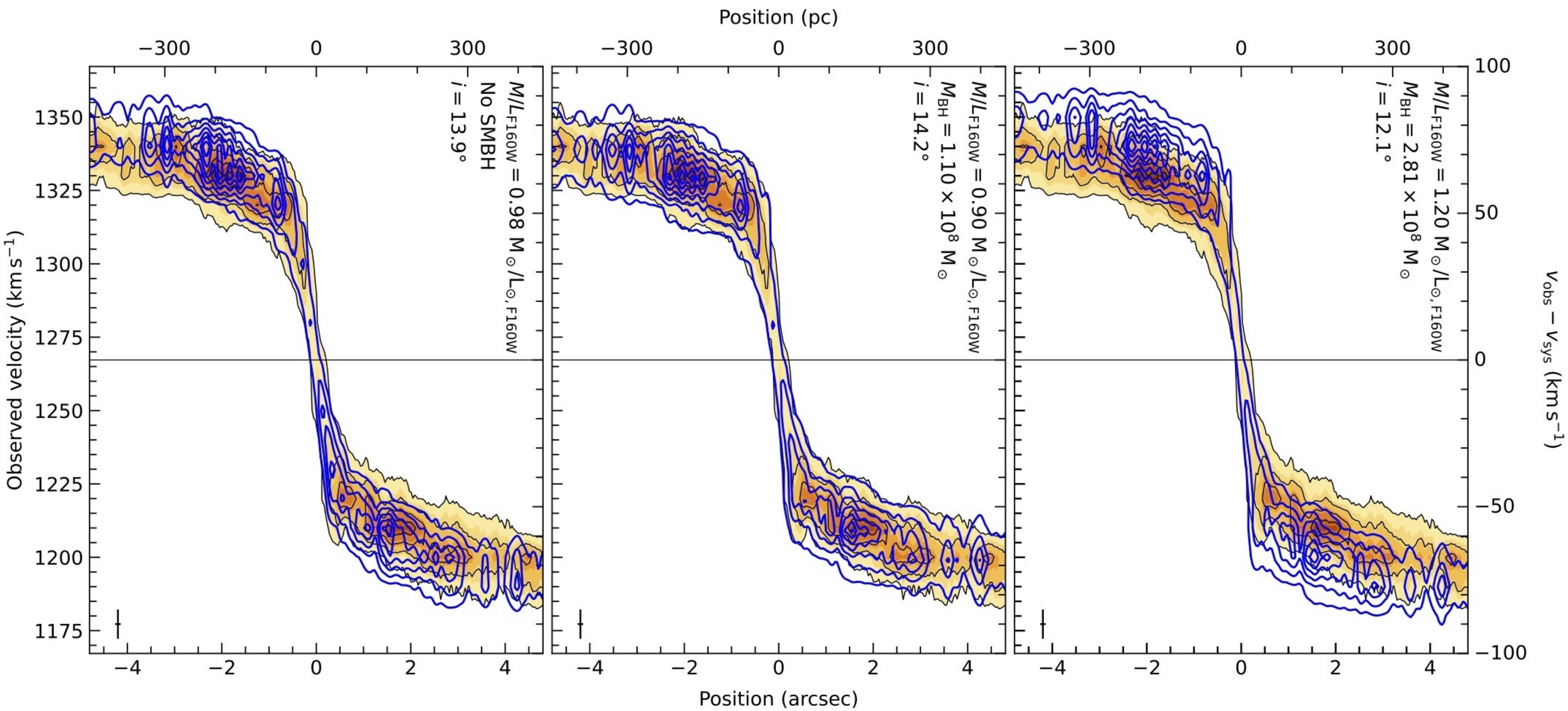

Figure 8. Inner part (radii $R \lesssim 5.0$ arcsec) of the observed kinematic major-axis PVD of NGC 1387 (orange scale with black contours), overlaid with the best-fitting no SMBH (left), free SMBH mass (centre) and overly-massive SMBH (right) model (blue contours), respectively. The SMBH mass, M/L and inclination of each model are listed in the top-right corner of each panel. An error bar is shown in the bottom-left corner of each panel, showing the size of the synthesised beam along the kinematic major axis and the channel width. The need for a central dark mass to fully account for the gas kinematics at all radii is clear.

Черная дыра – точно, как ожидалось

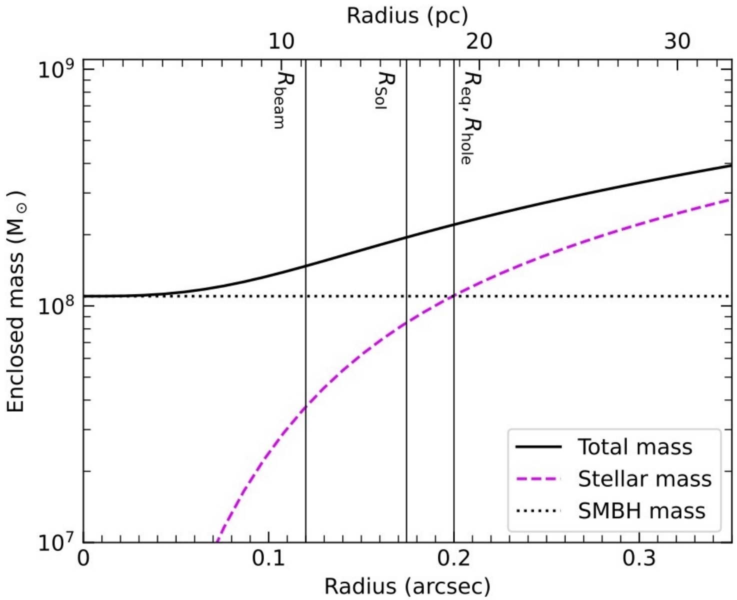

Figure 9. Cumulative mass function of NGC 1387, showing the relative contributions of the SMBH (black dotted line) and stars (magenta dashed line) to the total enclosed mass (black solid line). The three vertical black lines indicate the physical extent of the synthesised beam ($R_{\rm beam}$), the usually-defined radius of the SMBH sphere of influence ($R_{\rm SoI}$; adopting $\sigma_{\rm e}$ = 170.2 km s^{-1} and our best-fitting SMBH mass) and the approximate radius of the central hole ($R_{\rm hole}$) which is in this case the same as the radius of equal mass contribution ($R_{\rm eq}$).

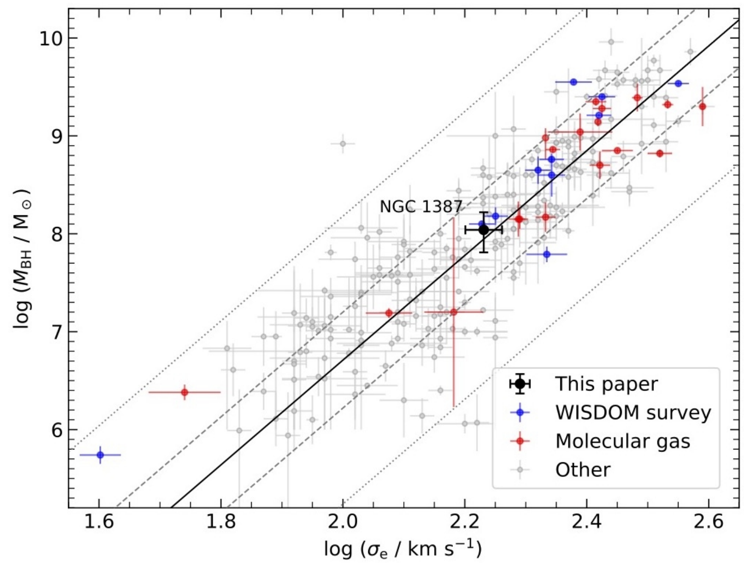

Figure 10. Black hole mass – stellar velocity dispersion relation obtained using stellar kinematic, ionised-gas kinematic, maser kinematic and active galactic nucleus reverberation mapping measurements (grey data points), as reported by van den Bosch (2016). Blue data points show measurements obtained using molecular gas kinematics by the WISDOM survey, while red data points show measurements obtained using molecular gas kinematics by other groups. The NGC 1387 measurement from this paper is shown as a black data point. Error bars denote 1σ uncertainties. The solid black line shows the best-fitting relation of van den Bosch (2016), while dashed and dotted grey lines show the 1σ and 3σ scatter of the relation, respectively.